Published in final edited form as:
Am J Drug Alcohol Abuse. 2013 November ; 39(6): 356–364. doi:10.3109/00952990.2013.818680.

Family History of Alcohol Use Disorders and Neuromaturation: A Functional Connectivity Study with Adolescents

A.D. Spadoni[1,2], **A.N. Simmons**[1,2], **T.T. Yang**[3], and **S.F. Tapert**[1,2]

[1] Veterans Affairs San Diego Healthcare System, San Diego, CA 92161

[2] University of California San Diego, La Jolla, CA, 92037

[3] University of California, San Francisco, CA, 94122

Abstract

BACKGROUND—A positive family history (FHP) of alcohol use disorders (AUD) is linked to increased risk for personal AUD, but the mechanisms behind this risk are unclear. Previous research suggests that a subtle neurodevelopmental lag in FHP adolescents may contribute to risk for future AUD.

METHODS—Functional magnetic resonance imaging (fMRI) response to a spatial working memory (SWM) task was examined for markers of neuromaturational delay in 85 youth with and without FHP. It was hypothesized that FHP adolescents (*n*=24, ages 12-14), as compared to matched FHN youth (*n*=26, ages 12-14), would show less similarity to brain connectivity observed in older adolescents (OA; *n*=35, ages 16-20) and that statistical comparison of SWM functional connectivity models would differentiate FHN and FHP youth. Structural equation modeling tested the fit of brain response connectivity between FH groups and against the OA model.

RESULTS—Patterns of connectivity were more similar between OA and FHN than FHP adolescents; FHP youth demonstrated higher association between right posterior and left frontal brain regions than FHN and OA youth. Comparison of FH groups indicated a significant difference on the pathway from the right superior parietal lobule to the left middle frontal gyrus.

CONCLUSIONS—These findings provide additional support for the notion of a neuromaturational lag in FHP youth. Protracted neuromaturation may be a mechanism by which FH increases risk for alcohol dependence, and this less mature neural connectivity pattern may provide a novel endophenotype for identifying youth at risk for drinking problems.

INTRODUCTION

Alcohol use remains prevalent in the youth of America, with 28% of youths ages 12 to 17 reporting past month alcohol use (1). One of the most robust risk factors for developing an alcohol use disorder (AUD) is a positive family history (FH) of AUD (2-9). Because many individuals with AUD are family history positive (FHP), understanding the neural characteristics of FHP youth may aid in the early identification of youth at greatest risk for developing AUD and facilitate early intervention development and implementation that could prevent the development of AUD in at risk youths.

Familial AUD has been linked to unique patterns of neuroanatomy (10, 11), neurocognition (12, 13), neurophysiology (14), and brain functioning (15). As some these neural markers

Corresponding Author: Susan Tapert, Ph.D. Department of Psychiatry University of California San Diego 3350 La Jolla Village Dr. Building 13, MC 116-B La Jolla CA 92161 TEL: (858) 552-8585 ext. 7563 FAX: (858) 552-7414 stapert@ucsd.edu.

are no longer detectable in FHP adults, such patterns have been theorized to be evidence of an inherited neurodevelopmental lag in FHP youth (16). For example, since amygdala and intracranial volume increase over childhood and adolescence, reduced volumes in FHP youth may indicate a developmental lag (12, 13). Also, the P300 component of the event-related potential has shown reduced amplitude in FHP children and adults (16) as well as in heavy drinkers (17), suggesting a potential endophenotype of alcoholism (18). This feature is most consistently displayed in FHP individuals under age 18, after which FHP individuals begin to resemble FHN peers, suggesting an inherited developmental lag (16). Finally, delayed maturation of postural sway (19) has also been implicated in FHP youth. These neural features, which appear to be more salient in youth, may confer greater risk for the development of future AUD.

Consistent with this theory, functional neuroimaging studies also suggest a potential neurobiological endophenotype that could increase risk for developing an AUD in youth with dense familial histories. For example, FHP youth demonstrated different patterns of brain response during tasks of inhibition (20), judging facial expressions (15), gambling (21), and in response to affective stimuli (22) than FHN peers. Furthermore, a positive FH was linked to greater activation of the right superior parietal cortex (23) and lentiform nucleus and insular region (24) during spatial working memory (SWM), and less activation during a simple vigilance condition relative to SWM in cingulate and medial frontal gyri (25). Less activation in multiple areas of the prefrontal cortex was also observed during verbal working memory (26). Finally, FHP compared to FHN youth have shown abnormal patterns of functional connectivity between prefrontal cortices with posterior parietal areas (27), prefrontal and cerebellar regions (28), and nucleus accumbens and posterior parietal and sensorimotor cortex (29). However, to our knowledge, there are no studies examining whether patterns of functional brain activation in FHP youth are consistent with a neurodevelopmental delay hypothesis.

Brain response during SWM may provide an opportunity to observe a hypothesized neurodevelopmental lag in FHP youth, as the developmental trajectory of frontoparietal pathways invoked to complete SWM tasks may be moderated by premorbid family history effects (18, 23, 30). Specifically, the underlying neural substrates of SWM appear to develop during adolescence, shifting more posterior and lateralizing to the right side, while the inferior parietal lobe becomes more important to task success (31-37). Thus, examination of FH effects on neural networks supporting SWM during the appropriate developmental window may elucidate whether a positive FH of AUD moderates the typical trajectory of neurodevelopment.

The current paper employs a structural equation modeling (SEM) approach to examine the influence of a positive FH of alcohol abuse on an *a priori* specified model of SWM in early adolescents, aged 12-14 years, and compares these patterns of functional connectivity to those of older adolescents (OA), aged 16-20, to help determine potential markers of neurodevelomental lag. We chose SEM to perform this path analysis instead of multivariate regression because it requires the *a priori* designation of hypothesis driven models (38) and provides multiple indices of overall model fit allowing for objective selection of optimal models. Specifically, this study tests the hypotheses that: 1) activation networks of FHN early adolescents will more closely resemble those of OA than will the FHP youth; and 2) statistical comparison of SWM functional connectivity models will differentiate FHN and FHP youth. These results will aid in determining neural risk factors for the future development of problem drinking and help inform the development of innovative treatments to prevent the development of AUD in at risk youths.

METHODS

Model specification

To test whether brain regions work together differently in youth with a positive FH of AUD, models of brain activity during SWM were created. The OA model was developed to include brain regions that best approximate patterns previously reported for older adolescents and adults in response to an SWM fMRI task (39-44)(Figure 1). Due to the constraints of the analytic approach, the model was made recursive (and thus unidirectional) to maximize our ability to test our hypotheses. Regions of interest (ROIs) included: 1) right inferior parietal lobule, 2) right superior parietal lobule, 3) right middle frontal gyrus, and 4) left middle frontal gyrus, based on evidence that these regions are a) integral to SWM functions (39-44), b) sensitive to shifts in cortical organization or change in strategies that accompany adolescent development (31-36, 45, 46), and c) susceptible to FH effects (30, 47, 48).

Participants

To create models of comparison, OA youth (*N*=35) between the ages of 16 and 20, 67% Caucasian, and 74% male (Table 1a), and early adolescents (*N*=50) between the ages of 12 and 14, 83% Caucasian, and 56% male (Table 1b), were sampled from two larger studies on neurocognition (R01 AA13419, and R01 DA021182). The early adolescent group was comprised of FHP (*n*=24) and FHN (*n*=26) groups that were statistically equivalent on parental education, annual salary, and pubertal development. All adolescents had minimal exposure to alcohol, cigarettes and marijuana (Tables 1a and 1b).

Biological parents' and grandparents' lifetime history of AUD was obtained from both parents and participant using the Family History Assessment Module screener (FHAM) (49) and Schuckit's Problem List (4). Most participants had 2 biological parents as informants, and all participants had at least one. Of the FHP group, 100% had a parent with an AUD history, 79% had a multigenerational history, 63% had a biological father with a history of AUD, 46% had a biological mother with a history of AUD, 8% had positive history in both parents, and one subject had a history of AUD solely in their biological mother. Of the OA group, 14% had a parent with an AUD history, and 11% had a multigenerational history. FHN youth had no history of any substance use disorder in parents or grandparents.

Subjects were excluded if they had a history of head injury with loss of consciousness >2 minutes, neurological or medical problems, learning disabilities, psychiatric disorder, current psychotropic medication use, significant maternal drinking or drug use during pregnancy, left-handedness, sensory deficits, MRI contraindications; and parental history of bipolar I, psychotic disorder, or antisocial personality disorder. The youth and participating family members were financially compensated for participation.

Mood assessments—State measures were collected at the time of scanning. Current level of depression was assessed with the Beck Depression Inventory (BDI) (50), which has been validated with 12 to 14 year-olds (51). The state portion of the Spielberger State-Trait Anxiety Inventory (52) was administered to ensure that youths were not experiencing any nervousness that could influence fMRI results (53).

Procedures

Scanning parameters—Early adolescent brain images were acquired on a 1.5 Tesla General Electric Signa LX scanner. A high-resolution structural image was collected in the sagittal plane using an inversion recovery prepared T1-weighted three-dimensional spiral fast-spin echo sequence (repetition time = 2,000 ms, echo time = 16 ms, field of view = 240

mm, resolution = 0.9375 mm × 0.9375 mm × 1.328 mm). Functional imaging was collected in the axial plane using T2*-weighted spiral gradient recall echo imaging (156 repetitions, repetition time = 3000 ms, echo time = 40 ms, flip angle = 90°, field of view = 240 mm, 20 continuous 7 mm slices, in-plane resolution = 1.875 mm × 1.875 mm).

OA images were acquired on a 3T General Electric Excite MR system with an 8-channel phase-array head coil (General Electric Medical System, Milwaukee, WI, USA). A high-resolution anatomical SPGR image was acquired sagittally (TR = 8 ms, TE = 3 ms, flip angle = 12°, 1 mm^3 voxels, FOV 240 mm, matrix interpolated to 256x256, slice thickness 1mm, 176 slices, bandwidth 31.25, acquisition time 7 minutes and 19 seconds). Functional imaging was collected in the axial plane using T2-weighted gradient echo imaging (156 repetitions, repetition time = 3000 ms, echo time = 30 ms, flip angle = 90°, field of view = 240 mm, 32 continuous 3.8 mm slices, matrix 64 × 64, in-plane resolution = 3.75 mm × 3.75 mm, total time 7 minutes 48 seconds). EPIs were unwarped with two field map acquisitions (each 1 minute and 8 seconds acquisition time; TR: 1000 ms, flip angle 60, FOV 240 mm, 32 contiguous axial slices each 3.8 mm thick, matrix 64 × 64, echo times 3.2 and 5.5 ms). Both groups completed the same SWM task (Figure 2), as previously described in detail (54).

Data Analysis and Statistics

Image processing—Data were processed and analyzed using Analysis of Functional NeuroImages (AFNI; afni.nimh.nih.gov) (55). Motion in the time series data was corrected by registering each acquisition to a selected repetition with an iterated least squares algorithm (56) to estimate three rotational and three displacement parameters for each participant. We excluded 1) all brain volumes where rigid motion exceeded 3mm (i.e., voxel width) allowing us to maintain a 90% power threshold, 2) and individuals whose performance on the SWM task fell outside 3 SD from the mean (n=3). An output file specifying adjustments made was used to control for spin history effects (57). In addition, applied adjustments were compared between groups, and correlated with the task reference vector to see if motion indices needed to be corrected in subsequent analyses.

The time series data were deconvolved with a reference vector that coded the hypothesized BOLD signal for the alternating task conditions across the time series of the task while covarying for linear trends and the degree of motion correction previously applied (58). The reference vector was convolved with a vector that modeled the typical hemodynamic response (59). All data were transformed into standardized space (60). The functional data were resampled into 3 mm cubic voxels, and a spatial smoothing Gaussian filter (FWHM = 5 mm) was applied. These steps resulted in a fit coefficient for each voxel, representing BOLD response to SWM relative to the vigilance baseline condition. A three-step process was used to identify relevant activations for analysis (61). First, a stereotaxic brain atlas (60) was used to define the a priori regions of interest (ROIs). Second, significant clusters of activation (α = .025; volume > 1,323 μL) were identified for each group using AFNI 3dttest within the ROIs. Third, the peak activation within each significant cluster was extracted for each participant, and screened for multivariate outliers and non-normal distribution. The final values represented each subject's maximal contrast between the SWM and baseline vigilance conditions.

SEM using EQS software (62) was used to examine the discrepancy between the hypothesis-driven path models specified for each group (Figure 1) by testing them against the observed data for the extracted ROI data. After good model fits were obtained, the importance of each path to overall model fit was examined by removing paths from the good fitting model one at a time with replacement and re-running the structural equation analysis (Table 3).

RESULTS

Behavioral performance and group membership

A 3-way ANOVA compared performance of group by SWM and vigilance conditions (Table 2). Tukey's post-hoc tests demonstrated that OA youth performed significantly better than FHN youth on all measures, and better than FHP on vigilance reaction time. FHP youth performed significantly better than FHN youth on SWM accuracy.

Model Fit in Young Adult Sample—The hypothesized model (Figure 1; left) fit the OA validation sample well (S-Bχ^2 [2, N=35]=1.85, p=.40 and descriptively (CFI=1.00, RMSEA= .00, $CI_{90\%}$ =.00-.33)). All standardized path coefficients were ranged from .356 to .767 and were statistically significant (ps<.05).

Model fit in FHN and FHP Adolescents samples—Covariance matrices for FHP and FHN early adolescents were generated and model fit indices when constrained to OA model were examined. The specified OA model did not fit either group statistically (FHN S-Bχ^2 [2, N=26]=6.153, p=.046; FHP S-Bχ^2 [2, N=24]=8.451, p=.015). The residual matrices for both groups indicated that the greatest amount of variance missing was from a bilateral connection between the right superior parietal lobule and the left middle frontal gyrus. The standardized residual was .40 in FHP and .28 in FHN, indicating greater variance unaccounted for in the FHP group. The addition of a bilateral path from the right superior parietal lobule and left middle frontal gyrus (Figure 3) greatly improved statistical fit (FHN SBχ^2 [1, N=26]=0.133, p=.716; FHP S-Bχ^2 [1, N=24]=0.891, p=.345) and was not statistically redundant (FHN RMSEA= 0.000 with $CI_{90\%}$ =.000-.392; FHP RMSEA = 0.000 with $CI_{90\%}$=.000-.528). However, the path from the right inferior parietal lobule and right middle frontal gyrus was not significant in either FH group of early adolescents. For FHN participants, the remaining standardized path coefficients were statistically significant (ps<.05) and ranged from .378 to .796. For the FHP group, the remaining loadings ranged from .326 to .734, indicating less good fit to the mature model.

Early Adolescent Model Modification

Deletion of the path from the right inferior parietal lobule to right middle frontal gyrus resulted in good overall fitting models for both groups (i.e., FHN S-Bχ^2 [2, N=26]=0.113, p=.945; FHP S-Bχ^2 [2, N=24]=2.124, p=.346) was statistically parsimonious and more likely to replicate (FHN RMSEA= 0.000 with $CI_{90\%}$ =.000-.149; FHP RMSEA = 0.000 with $CI_{90\%}$ =.000-.387). Standardized path coefficients were statistically significant (ps<.05) across groups and ranged from .326 to .734 and .411 to .804, respectively (Figure 4).

Group differences

Partial model invariance was established for OA from early adolescent, and between FH groups. Although three of 4 pathways in each groups' final model (right middle frontal gyrus to left middle frontal gyrus, right superior parietal lobule to right middle frontal gyrus, and right inferior parietal lobule to right superior parietal lobule) (ps>.172) were statistically comparable, comparison of FH groups on their shared final model indicated invariance on the pathway added from the right superior parietal lobule to the left middle frontal gyrus (χ^2 =4.75, p=.029; dashed line Figure 4). This pathway was redundant in the OA model and not included in the final model. Of note, removal of the right superior parietal lobule to left middle frontal gyrus pathway, the connection that was statistically different between FH groups, decreased overall model fit much more in FHP than FHN models, underscoring the magnitude of group differences (Table 3). When SWM accuracy scores were included in each samples' model of best fit, as related to each region of interest, and re-run one relationship at a time, increased SWM accuracy scores were significantly and negatively

related to activation of the right superior parietal node in the FHP sample (FHP S-Bχ^2 [5, N=24]=7.135, p=.211, RMSEA= 0.000 with $CI_{90\%}$ =.000-.279; r^2=.16). Covariance of SWM performance across sample comparisons did not affect the previously described outcomes. In consideration of the small effect size of the path in the FHP group, differences in sample size, and invariance between groups, the influence of SWM accuracy on the overall model fit was judged to be insignificant. Taken together, these results suggest that age and FH status was shown to moderate the neural networks supporting successful SWM completion.

DISCUSSION

Consistent with our hypotheses, we demonstrated that 1) youth without dense family histories of AUD produced a network of brain activity that resembled the OA model more than that of the FHP comparison group as illustrated by overall fit indices, and 2) FHP youth demonstrated a statistically significant stronger regression coefficient for the bilateral pathway between the right superior parietal lobule to left middle frontal gyrus. Removal of the bilateral pathway from the FHP model decreased overall fit indices much more than when it was removed from the FHN group, underscoring the extent of group differences. The difference between FHN and FHP remained unchanged after controlling for SWM performance, which was slightly superior in FHP youth, suggesting that this difference is not mediated by SWM performance. These data contribute to the growing evidence that familial history of AUD may influence neurobehavioral correlates and thus contribute to increased rates of problem drinking in FHP youth.

These findings provide evidence in support of the neurodevelopmental delay hypothesis, which suggests that protracted neuromaturation is a potential mechanism through which a positive FH increases risk for alcohol dependence (16). Developmental literature suggests that with increasing skill in cognitive resources such as inhibition, processing speed, and working memory, children and adolescents improve their mastery in tasks that require these component processes (63, 64). Mastery and integration of each subcomponent improves overall cognitive control of behavior. A subtle deficit in one or more of these cognitive elements may lead to reduced complex cognitive control and postponed mastery of interdependent neurocognitive functions. Therefore, an adolescent with a subtle lag in fronto-parietal neuromaturation may also suffer a concomitant delay in achieving inhibitory control (65-68). Therefore, greater similarity of FHN neural networks to those in healthy older adolescents may illustrate such an increased vulnerability.

To our knowledge there are 3 manuscripts that have examined functional connectivity in youth with and without familial AUD. Wetherill et al., 2012 used seed voxel analyses and found FHP youth (aged 12-14) demonstrated relatively less functional connectivity between frontal and parietal regions during a visual working memory (VWM) task (27). Herting et al., 2011 also used seed voxel analyses and demonstrated reduced fronto-cellebellar connectivity within FHP youth (aged 11-15) during rest (28). Finally Weliand et al., 2013 used psychophysiological interaction analyses and found increased nucleus accumbens connectivity with posterior parietal and sensorimotor areas during incentive anticipation in FHP youth (aged 18-22 years; some with prior substance use disorders (SUD))(29). Because of different task demands, regions of interest, analytic approaches (e.g., multivariate vs. univariate), dissimilar age groups, and presence of SUD, it is difficult to draw conclusions from this literature. Interestingly, the most comparable study by Wetherill et al., 2011 found decreased connectivity between bilateral frontal and parietal regions during VWM in FHP youth while we found increased connectivity between similar regions during SWM. One potential reason for this divergence may be the sensitivity of specific neural substrates to detect FH, or neurodevelopmental, effects. While the critical neural substrates of visual

working memory are located in the ventrolateral prefrontal cortex, spatial working memory relies on a more superior and dorsal stream (69) which was has been demonstrated to develop in anticipated manner (31-36, 45, 46). Therefore, less connectivity between superior parietal and dorsolateral prefrontal cortices during visual working memory in FHP youth may not have the same implications as a similar pattern during spatial working memory demands. Regardless, our findings are consistent with these in that a familial history of AUD moderated functional connectivity.

These data should be considered in light of several limitations. First, the younger cohort was scanned on a 1.5T magnet using a spiral acquisition, while the older cohort was imaged on a 3T system using an EPI acquisition. Although data were collected on disparate field strengths the relative relationships between the regions of interest should be proportionately scaled (70). Also, reported differences in functional connectivity across magnet strengths appear to be more pronounced in non-task related demands (i.e., resting) (71). Importantly, comparisons across field strength *and* technique suggest comparable signal dropout between 1.5T spiral and 3T EPI acquisitions in regions other than the frontal orbital cortex (72). Second, the demographic makeup of our sample may attenuate FH effects on functional connectivity. Most participants are from relatively affluent areas of San Diego and have highly educated parents. Genetic risk for AUD is less likely to be expressed in such environments (73). Sampling a greater number of participants with increased risks for AUD might increase the likelihood of finding FH effects on neuromaturation. Third, our OA group was not wholly comprised of FHN youth. Our FH-mixed OA group may have diminished our ability to detect FH effects. Fourth, as these data are cross-sectional in nature, longitudinal follow-up data in early adulthood will be needed to fully test the neuromaturational lag hypothesis, and to examine whether the FHP youth do indeed catch up to the FHN youth. Fifth, failure to include bidirectional relationships between regions of interest limits our ability to accurately represent neural networks.

The influence of protracted neuromaturation within a larger constellation of risk factors for AUD has yet to be understood. Longitudinal studies are needed to address the contribution of neurodevelopment in order to understand the interplay of factors predicting AUD and to help reduce global rates of alcohol-related disease.

REFERENCES

1. Johnston, LD.; O'Malley, PM.; Bachman, JG.; Schulenberg, JE. Monitoring the Future national survey results on drug use, 1975-2011. Vol. 760. Institute for Social Research, The University of Michigan; Ann Arbor: 2012.
2. Cloninger CR, Sigvardsson S, Reich T, Bohman M. Inheritance of risk to develop alcoholism. NIDA Res Monogr. 1986; 66:86–96. [PubMed: 3106820]
3. Goodwin DW. Alcoholism and heredity. A review and hypothesis. Arch Gen Psychiatry. 1979; 36(1):57–61. [PubMed: 367310]
4. Schuckit MA. Genetics and the risk for alcoholism. Jama. 1985; 254(18):2614–2617. [PubMed: 4057470]
5. Sartor CE, Lynskey MT, Heath AC, Jacob T, True W. The role of childhood risk factors in initiation of alcohol use and progression to alcohol dependence. Addiction. 2007; 102(2):216–225. [PubMed: 17222275]
6. Liu IC, Blacker DL, Xu R, Fitzmaurice G, Tsuang MT, Lyons MJ. Genetic and environmental contributions to age of onset of alcohol dependence symptoms in male twins. Addiction. 2004; 99(11):1403–1409. [PubMed: 15500593]
7. King SM, Keyes M, Malone SM, Elkins I, Legrand LN, Iacono WG, McGue M. Parental alcohol dependence and the transmission of adolescent behavioral disinhibition: a study of adoptive and non-adoptive families. Addiction. 2009; 104(4):578–586. [PubMed: 19215604]

8. Capone C, Wood MD. Density of familial alcoholism and its effects on alcohol use and problems in college students. Alcohol Clin Exp Res. 2008; 32(8):1451–1458. [PubMed: 18564105]
9. Sartor CE, Agrawal A, Lynskey MT, Bucholz KK, Heath AC. Genetic and environmental influences on the rate of progression to alcohol dependence in young women. Alcohol Clin Exp Res. 2008; 32(4):632–638. [PubMed: 18331380]
10. Gilman JM, Bjork JM, Hommer DW. Parental Alcohol Use and Brain Volumes in Early-and Late-Onset Alcoholics. Biol Psychiatry. 2007; 15:15.
11. Hill SY, De Bellis MD, Keshavan MS, Lowers L, Shen S, Hall J, Pitts T. Right amygdala volume in adolescent and young adult offspring from families at. Biol Psychiatry. 2001; 49(11):894–905. [PubMed: 11377407]
12. Corral MM, Holguin SR, Cadaveira F. Neuropsychological characteristics in children of alcoholics: familial density. J Stud Alcohol. 1999; 60(4):509–513. [PubMed: 10463807]
13. Corral M, Holguin SR, Cadaveira F. Neuropsychological characteristics of young children from high-density alcoholism. J Stud Alcohol. 2003; 64(2):195–199. [PubMed: 12713192]
14. Begleiter H, Porjesz B, Bihari B, Kissin B. Event-related brain potentials in boys at risk for alcoholism. Science. 1984; 225(4669):1493–1496. [PubMed: 6474187]
15. Hill SY, Kostelnik B, Holmes B, Goradia D, McDermott M, Diwadkar V, Keshavan M. fMRI BOLD response to the eyes task in offspring from multiplex alcohol dependence families. Alcohol Clin Exp Res. 2007; 31(12):2028–2035. [PubMed: 18034695]
16. Hill SY, Shen S, Locke J, Steinhauer SR, Konicky C, Lowers L, Connolly J. Developmental delay in P300 production in children at high risk for developing alcohol-related disorders. Biological Psychiatry. 1999; 46(7):970–981. [PubMed: 10509180]
17. Porjesz B, Begleiter H. HUMAN EVOKED BRAIN POTENTIALS AND ALCOHOL. Alcoholism-Clinical and Experimental Research. 1981; 5(2):304–317.
18. Hesselbrock V, Begleiter H, Porjesz B, O'Connor S, Bauer L. P300 event-related potential amplitude as an endophenotype of alcoholism-evidence from the collaborative study on the genetics of alcoholism. J Biomed Sci. 2001; 8(1):77–82. [PubMed: 11173979]
19. Hill SY, et al. Developmental changes in postural sway in children at high and low risk for developing alcohol-related disorders. Biological Psychiatry. 2000; 47:501511.
20. Schweinsburg AD, Paulus MP, Barlett VC, Killeen LA, Caldwell LC, Pulido C, Brown SA, Tapert SF. An FMRI study of response inhibition in youths with a family history of alcoholism. Ann N Y Acad Sci. 2004; 1021:391–394. [PubMed: 15251915]
21. Acheson A, Robinson JL, Glahn DC, Lovallo WR, Fox PT. Differential activation of the anterior cingulate cortex and caudate nucleus during a gambling simulation in persons with a family history of alcoholism: studies from the Oklahoma Family Health Patterns Project. Drug Alcohol Depend. 2009; 100(1-2):17–23. [PubMed: 19026496]
22. Heitzeg MM, Nigg JT, Yau WY, Zubieta JK, Zucker RA. Affective circuitry and risk for alcoholism in late adolescence: differences in frontostriatal responses between vulnerable and resilient children of alcoholic parents. Alcohol Clin Exp Res. 2008; 32(3):414–426. [PubMed: 18302724]
23. Seghete KLM, Cservenka A, Herting MM, Nagel BJ. Atypical Spatial Working Memory and Task-General Brain Activity in Adolescents with a Family History of Alcoholism. Alcoholism-Clinical and Experimental Research. 2013; 37(3):390–398.
24. Norman AL, O'Brien JW, Spadoni AD, Tapert SF, Jones KL, Riley EP, Mattson SN. A functional magnetic resonance imaging study of spatial working memory in children with prenatal alcohol exposure: contribution of familial history of alcohol use disorders. Alcohol Clin Exp Res. 2013; 37(1):132–140. [PubMed: 23072431]
25. Spadoni AD, Norman AL, Schweinsburg AD, Tapert SF. Effects of family history of alcohol use disorders on spatial working memory BOLD response in adolescents. Alcoholism-Clinical and Experimental Research. 2008; 32(7):1135–1145.
26. Cservenka A, Herting MM, Nagel BJ. Atypical frontal lobe activity during verbal working memory in youth with a. Drug Alcohol Depend. 2012; 123(1-3):98–104. [PubMed: 22088655]

27. Wetherill RR, Bava S, Thompson WK, Boucquey V, Pulido C, Yang TT, Tapert SF. Frontoparietal connectivity in substance-naive youth with and without a family. Brain Res. 2012; 1432:66–73. [PubMed: 22138427]
28. Herting MM, Fair D, Nagel BJ. Altered fronto-cerebellar connectivity in alcohol-naive youth with a family. Neuroimage. 2011; 54(4):2582–2589. [PubMed: 20970506]
29. Weiland BJ, Welsh RC, Yau WY, Zucker RA, Zubieta JK, Heitzeg MM. Accumbens functional connectivity during reward mediates sensation-seeking and. Drug Alcohol Depend. 2013; 128(1-2):130–139. [PubMed: 22958950]
30. Rangaswamy M, Porjesz B, Ardekani BA, Choi SJ, Tanabe JL, Lim KO, Begleiter H. A functional MRI study of visual oddball: evidence for frontoparietal dysfunction. Neuroimage. 2004; 21(1): 329–339. [PubMed: 14741671]
31. Nelson CA, Monk CS, Lin J, Carver LJ, Thomas KM, Truwit CL. Functional neuroanatomy of spatial working memory in children. Developmental Psychology. 2000; 36(1):109–116. [PubMed: 10645748]
32. Schweinsburg AD, Nagel BJ, Tapert SF. fMRI reveals alteration of spatial working memory networks across adolescence. J Int Neuropsychol Soc. 2005; 11(5):631644.
33. Thomas KM, King SW, Franzen PL, Welsh TF, Berkowitz AL, Noll DC, Birmaher V, Casey BJ. A developmental functional MRI study of spatial working memory. NeuroImage. 1999; 10(3 Pt 1): 327–338. [PubMed: 10458945]
34. Klingberg T, Forssberg H, Westerberg H. Increased brain activity in frontal and parietal cortex underlies the development of visuospatial working memory capacity during childhood. J Cogn Neurosci. 2002; 14(1):1–10. [PubMed: 11798382]
35. Klingberg T. Development of a superior frontal-intraparietal network for visuospatial working memory. Neuropsychologia. 2006; 44(11):2171–2177. [PubMed: 16405923]
36. Thomason ME, Race E, Burrows B, Whitfield-Gabrieli S, Glover GH, Gabrieli JD. Development of spatial and verbal working memory capacity in the human brain. J Cogn Neurosci. 2009; 21(2): 316–332. [PubMed: 18510448]
37. Pessoa L, Gutierrez E, Bandettini P, Ungerleider L. Neural correlates of visual working memory: fMRI amplitude predicts task performance. Neuron. 2002; 35(5):975–987. [PubMed: 12372290]
38. Friston KJ. Functional and Effective Connectivity: A Synthesis. Human brain mapping. 1994; 2:56–78.
39. Courtney SM, Petit L, Maisog JM, Ungerleider LG, Haxby JV. An area specialized for spatial working memory in human frontal cortex. Science. 1998; 279:1347–1351. [PubMed: 9478894]
40. Goldman-Rakic PS. Circuitry of primate prefrontal cortex and regulation of behavior by representational memory. Handbook of physiology, the nervous system, higher functions of the brain. 1987; 5:373–417.
41. van Asselen M, Kessels RP, Neggers SF, Kappelle LJ, Frijns CJ, Postma A. Brain areas involved in spatial working memory. Neuropsychologia. 2006; 44(7):1185–1194. [PubMed: 16300806]
42. Ricciardi E, Bonino D, Gentili C, Sani L, Pietrini P, Vecchi T. Neural correlates of spatial working memory in humans: a functional magnetic. Neuroscience. 2006; 139(1):339–349. [PubMed: 16324793]
43. McCarthy G, Puce A, Constable RT, Krystal JH, Gore JC, Goldman-Rakic P. Activation of human prefrontal cortex during spatial and nonspatial working. Cereb Cortex. 1996; 6(4):600–611. [PubMed: 8670685]
44. Thomas KM, King SW, Franzen PL, Welsh TF, Berkowitz AL, Noll DC, Birmaher V, Casey BJ. A developmental functional MRI study of spatial working memory. Neuroimage. 1999; 10(3 Pt 1): 327–338. [PubMed: 10458945]
45. Edin F, Macoveanu J, Olesen P, Tegner J, Klingberg T. Stronger synaptic connectivity as a mechanism behind development of working memory-related brain activity during childhood. J Cogn Neurosci. 2007; 19(5):750–760. [PubMed: 17488202]
46. Casey BJ, Trainor RJ, Orendi JL, Schubert AB, Nystrom LE, Giedd JN, Castellanos FX, Haxby JV, Noll DC, Cohen JD, Forman SD, Dahl RE, Rapoport JL. A developmental functional MRI study of prefrontal activation during performance of a Go-No-Go task. Journal of Cognitive Neuroscience. 1997; 9:835–847. [PubMed: 23964603]

47. Mackiewicz Seghete KL, Cservenka A, Herting MM, Nagel BJ. Atypical Spatial Working Memory and Task-General Brain Activity in Adolescents. Alcohol Clin Exp Res. 2012
48. Hesselbrock V, Begleiter H, Porjesz B, O'Connor S, Bauer L. P300 event-related potential amplitude as an endophenotype of. J Biomed Sci. 2001; 8(1):77–82. [PubMed: 11173979]
49. Andreasen NC, Rice J, Endicott J, Reich T, Coryell W. The family history approach to diagnosis. How useful is it? Arch Gen Psychiatry. 1986; 43(5):421–429. [PubMed: 3964020]
50. Beck AT, Ward CH, Medelson M, Mock J, Erbaugh J. An inventory for measuring depression. Arch Gen Psychiatry. 1961; 4:561–571. [PubMed: 13688369]
51. Steer RA, Kumar G, Ranieri WF, Beck AT. Use of the Beck Depression Inventory-II with adolescent psychiatric outpatients. Journal of Psychopathology and Behavioral Assessment. 1998; 20(2)
52. Arnau RC, Meagher MW, Norris MP, Bramson R. Psychometric evaluation of the Beck Depression Inventory-II with primary care medical patients. Health Psychol. 2001; 20(2):112–119. [PubMed: 11315728]
53. Harris, GJ.; Hoehn-Saric, R., editors. Functional neuroimaging in biological psychiatry. Greenwich, CT: 1995.
54. Kindermann SS, Brown GG, Zorrilla LE, Olsen RK, Jeste DV. Spatial working memory among middle-aged and older patients with schizophrenia. Schizophr Res. 2004; 68(2-3):203–216. [PubMed: 15099603]
55. Brown SA, Christiansen BA, Goldman MS. The Alcohol Expectancy Questionnaire: an instrument for the assessment of adolescent and adult alcohol expectancies. J Stud Alcohol. 1987; 48(5):483–491. [PubMed: 3669677]
56. Cox RW, Jesmanowicz A. Real-time 3D image registration for functional MRI. Magn Reson Med. 1999; 42(6):1014–1018. [PubMed: 10571921]
57. Friston KJ, Williams S, Howard R, Frackowiak RS, Turner R. Movement-related effects in fMRI time-series. Magn Reson Med. 1996; 35(3):346–355. [PubMed: 8699946]
58. Bandettini PA, Jesmanowicz A, Wong EC, Hyde JS. Processing strategies for time-course data sets in functional MRI of the human brain. Magnetic Resonance in Medicine. 1993; 30:161–173. [PubMed: 8366797]
59. Cohen MS. Parametric analysis of fMRI data using linear systems methods. NeuroImage. 1997; 6(2):93–103. [PubMed: 9299383]
60. Talairach, J.; Tournoux, P. Three-dimensional proportional system: An approach to cerebral imaging. Thieme; New York: 1988. Coplanar stereotaxic atlas of the human brain..
61. Stricker JL, Brown GG, Wetherell LA, Drummond SP. The impact of sleep deprivation and task difficulty on networks of fMRI brain. J Int Neuropsychol Soc. 2006; 12(5):591–597. [PubMed: 16961940]
62. Bentler, PM.; Wu, EJC. EQS for Windows User's Guide. Multivariate Software, Inc.; Encino, CA.: 1995.
63. Luna B, Garver KE, Urban TA, Lazar NA, Sweeney JA. Maturation of cognitive processes from late childhood to adulthood. Child Dev. 2004; 75(5):1357–1372. [PubMed: 15369519]
64. Luna B, Thulborn KR, Munoz DP, Merriam EP, Garver KE, Minshew NJ, Keshavan MS, Genovese CR, Eddy WF, Sweeney JA. Maturation of widely distributed brain function subserves cognitive development. NeuroImage. 2001; 13(5):786–793. [PubMed: 11304075]
65. Porjesz B, Rangaswamy M, Kamarajan C, Jones KA, Padmanabhapillai A, Begleiter H. The utility of neurophysiological markers in the study of alcoholism. Clin Neurophysiol. 2005; 116(5):993–1018. [PubMed: 15826840]
66. Tarter RE. Are there inherited behavioral traits that predispose to substance abuse? J Consult Clin Psychol. 1988; 56(2):189–196. [PubMed: 3286703]
67. McGue M, Slutske W, Taylor J, Iacono WG. Personality and substance use disorders: I. Effects of gender and alcoholism subtype. Alcohol Clin Exp Res. 1997; 21(3):513520.
68. Cloninger CR, Sigvardsson S, Bohman M. Childhood personality predicts alcohol abuse in young adults. Alcohol Clin Exp Res. 1988; 12(4):494–505. [PubMed: 3056070]

69. Courtney SM, Ungerleider LG, Keil K, Haxby JV. Object and spatial visual working memory activate separate neural systems in human cortex. Cerebral Cortex. 1996; 6:39–49. [PubMed: 8670637]

70. van der Zwaag, W.; Francis, S.; Head, K.; Peters, A.; Gowland, P.; Morris, P.; Bowtell, R. Neuroimage. Vol. 47. United States: 2009. fMRI at 1.5, 3 and 7 T: characterising BOLD signal changes.; p. 1425-1434.

71. Hale JR, Brookes MJ, Hall EL, Zumer JM, Stevenson CM, Francis ST, Morris PG. Comparison of functional connectivity in default mode and sensorimotor networks at 3 and 7T. MAGMA. 2010; 23(5-6):339–349. [PubMed: 20625794]

72. Winter JD, Poublanc J, Crawley AP, Kassner A. Comparison of spiral imaging and SENSE-EPI at 1.5 and 3.0 T using a controlled cerebrovascular challenge. J Magn Reson Imaging. 2009; 29(5): 1206–1210. [PubMed: 19388098]

73. Sigvardsson S, Bohman M, Cloninger CR. Replication of the Stockholm Adoption Study of alcoholism. Confirmatory cross-fostering analysis. Arch Gen Psychiatry. 1996; 53(8):681–687. [PubMed: 8694681]

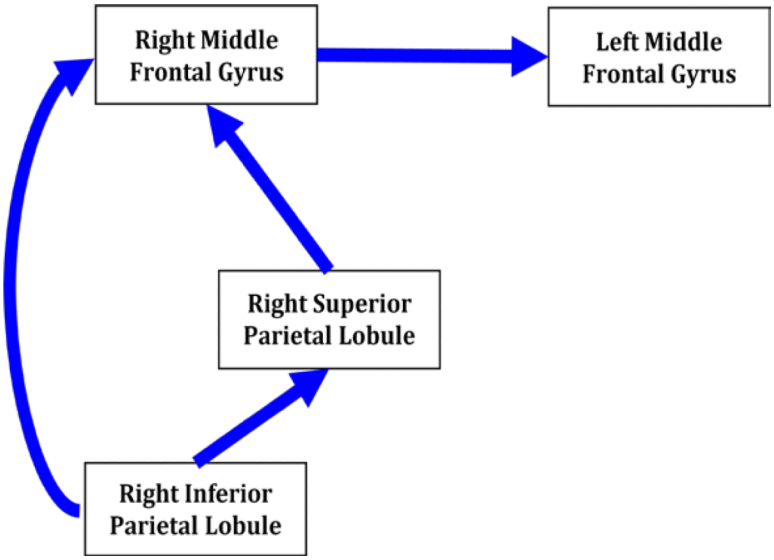

Figure 1.
Hypothesized Model of Functional Connectivity for older adolescents to be validated and compared to family history groups. The model of brain activity during spatial working memory was developed to include brain regions that best approximate patterns previously reported for older adolescents and adults in response to a spatial working memory imaging task. Regions of interest (ROIs) included: 1) right inferior parietal lobule, 2) right superior parietal lobule, 3) right middle frontal gyrus, and 4) left middle frontal gyrus.

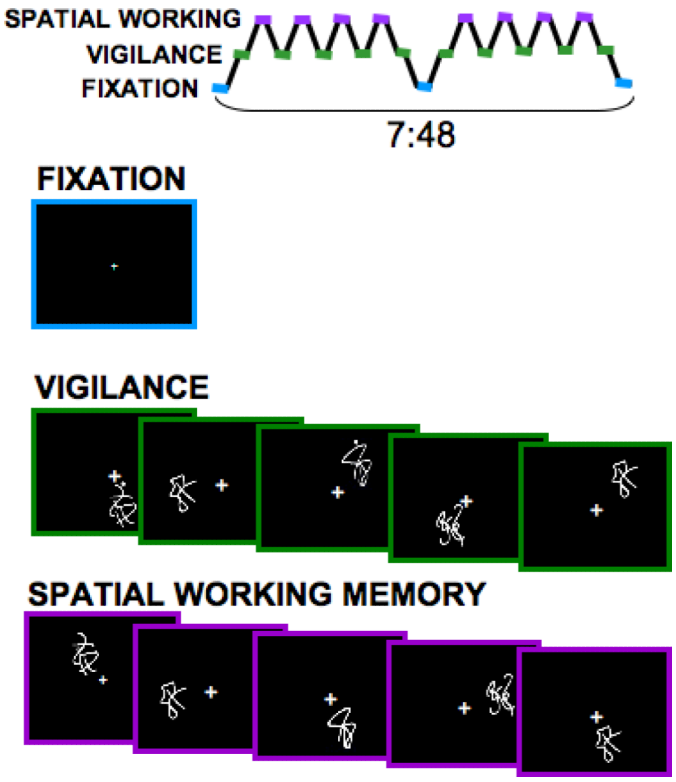

Figure 2.
Spatial working memory task design. The spatial working memory task consists of 18 20-sec blocks alternating between experimental (spatial working memory) and baseline (vigilance) conditions. In both conditions, stimuli were presented for 1000 ms, and each interstimulus interval is 1000 ms (20 sec/block, repetition time (TR) = 3000 ms, 156 repetitions).

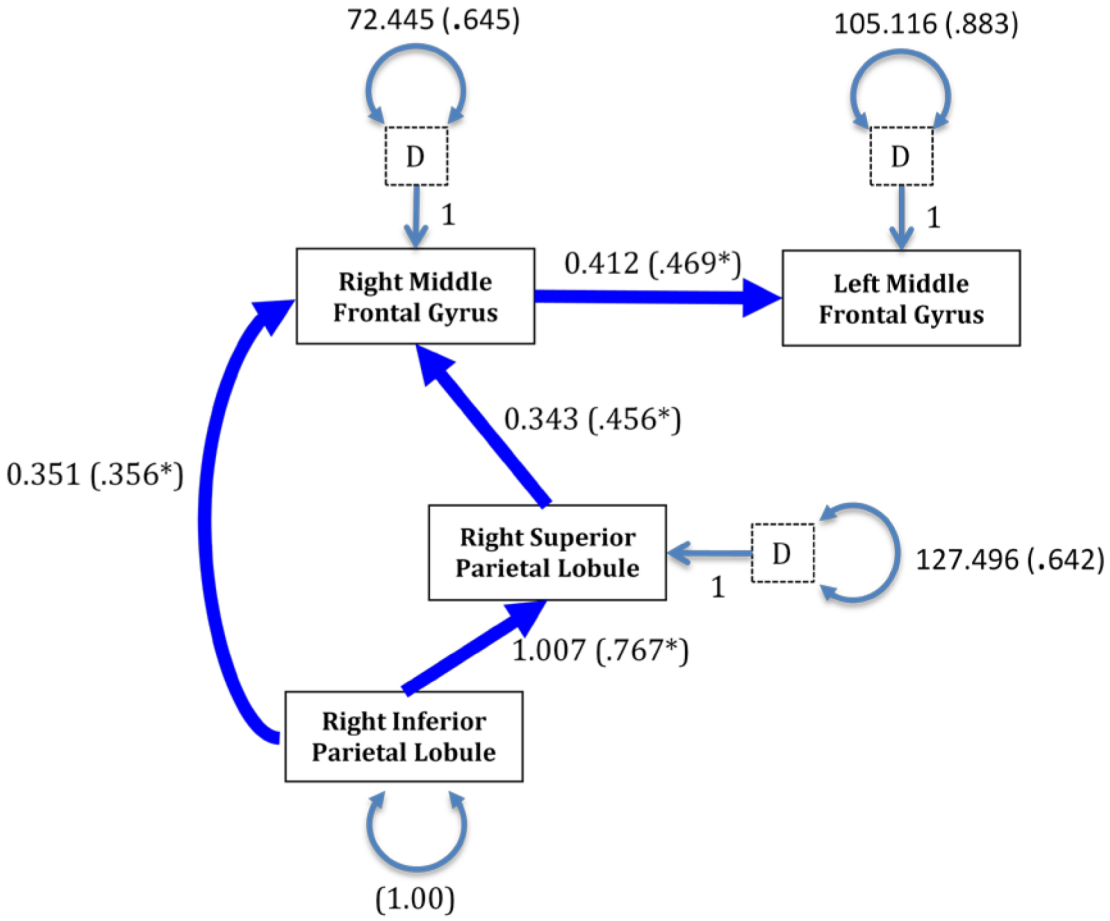

Effect size per path	(r^2)
Right middle frontal gyrus → Right superior parietal lobule → Left middle frontal gyrus	.584
Right middle frontal gyrus → Right superior parietal lobule	.220
Right superior parietal lobule → Right inferior parietal lobule	.588

Figure 3.
The results of fitting the covariance matrix to the proposed model in OA youth. Pathways labeled with unstandardized (and standardized in parentheses) coefficients (p<.05) and disturbances (D) with standard error terms for endogenous variables.

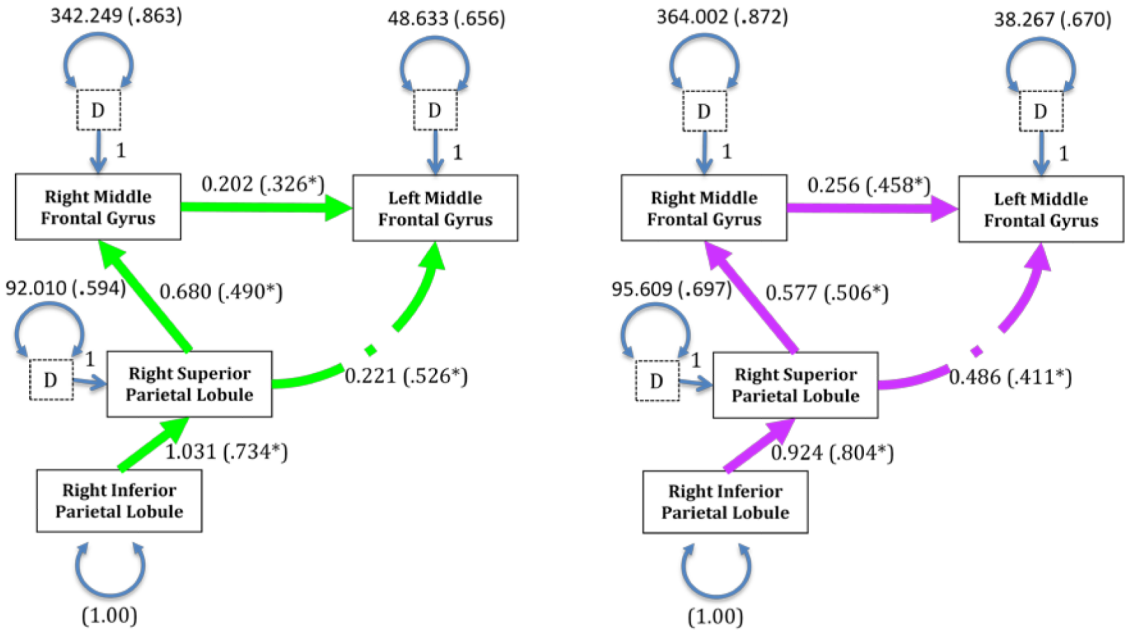

Effect size per path (r^2)	FHN	FHP
Right middle frontal gyrus → Right superior parietal lobule → Left middle frontal gyrus	.569	.552
Right middle frontal gyrus → Right superior parietal lobule	.256	.240
Right superior parietal lobule → Right inferior parietal lobule	.647	.539

Figure 4.
Best fitting FHN youth mode (LEFT); Best fitting FHP youth model (RIGHT); Pathways labeled with unstandardized (and standardized in parentheses) coefficients ($p<.05$) and disturbances (D) with standard error terms for endogenous variables.

Table 1a

Characteristics of older adolescent (OA) participants (*N*=35)

Variable	**M (*SD*) or %**
Sex (% Male)	74%
Age in years (range 16-20)	17.69 (1.07)
Ethnicity (% Caucasian)	67%
Conduct disorder diagnosis	0%
Father education	15.12 (3.27)
Mother education	14.35 (3.64)
Parental annual salary ($K)	116.00 (71.41)
CBCL internalizing *T*-score	44.66 (3.79)
CBCL externalizing *T*-score	44.23 (4.57)
Beck Depression Inventory total	11.00 (2.39)
Spielberger State Anxiety *T*-score	38.03 (7.94)
Lifetime uses of alcohol	1.86 (9.23)
Maximum drinks per episode last 3 months	4.00 (0.34)
Number of cigarettes past month	0.54 (3.21)
Lifetime uses of marijuana	0.54 (1.27)

Table 1b

Characteristics of early adolescent participants (*N*=50)

ANOVA and Chi-square comparing FH across categories				
Variable	**FHN *n*=26 M (*SD*) or %**	**FHP *n*=24 M (*SD*) or %**	***F*/χ^2**	***p***
Sex (% Male)	46%	67%	2.15	.14
Age in years (range 12-14)	13.16 (0.82)	13.25 (0.86)	.17	.70
Boys' age in years	13.50 (0.68)	13.34 (0.85)	1.02	.32
Pubertal Development Scale				
Girls (*n*=24)	3.20 (1.15)	3.13 (0.64)	.29	.87
Boys (*n*=28)	2.38 (0.77)	2.88 (0.72)	3.14	.09
Ethnicity (% Caucasian)	79%	88%	.72	.40
Mother education	15.75 (1.82)	14.63 (2.34)	3.81	.06
Father education	16.64 (1.83)	15.64 (2.50)	2.70	.11
Parental annual salary ($K)	127.27 (53.46)	125.38 (94.05)	.01	.93
CBCL internalizing *T*-score	45.87 (6.20)	47.38 (7.29)	.61	.44
CBCL externalizing *T*-score	44.93 (4.60)	46.87 (6.22)	1.55	.22
Beck Depression Inventory total	3.04 (3.35)	3.13 (3.39)	.01	.93
Spielberger State Anxiety *T*-score	27.96 (6.56)	30.67 (7.84)	1.83	.18
Lifetime uses of alcohol	0.39 (1.07)	0.63 (1.41)	.46	.50
Maximum drinks per episode	4.00	5.00	.09	.77
Lifetime uses of cigarettes	0.11 (0.32)	0.04 (0.21)	.69	.41
Lifetime uses of marijuana	0.18 (0.67)	0.22 (0.67)	.04	.84

* $p < .05$

Table 2

SWM performance of adolescent and young adult participants across SWM and vigilance conditions.

	FHN (*n*=26) M (*SD*) %	**FHP (*n*=24) M (*SD*) %**	**OA (*n*=35) M(*SD*) %**	***F (p)***
Vigilance accuracy (%)*	95.52 (2.13)	95.63 (2.17)	96.70 (1.49)	3.34 (.04)
Vigilance reaction time (ms)*	656.32 (60.94)	654.42 (53.67)	605.50 (62.76)	5.60 (.01)
SWM accuracy*	88.29 (7.62)	93.23 (4.23)	92.79 (5.01)	6.63 (.00)
SWM reaction time (ms)*	622.67 (77.32)	576.38 (74.92)	558.49 (64.16)	5.68 (.01)

* $p < .05$

Table 3

Summary of Goodness of Fit Statistics: Overall fit indices for each group's final best fitting model and respective changes with removal of each pathway.

Model	S-B χ^2	*p*-value	df	¥AIC	¥CFI	SRMR	¥RMSEA	¥RMSEA90%CI	Δ¥S-Bχ^2	Δdf	Δ¥CFI	ΔAIC
OA best fit	1.85	.40	2	−2.15	1.00	.03	.00	.00 - .33	--	--	--	--
Lmfg → Rmfg	--	--	0	--	--	--	--	--	--	--	--	--
Rspl → Rmfg	9.56	.02	3	3.56	.83	.08	.25	.08 - .44	7.34*	−1	−.17	5.71
Ripl → Rmfg	5.91	.12	3	−.09	.92	.06	.17	.00 - .37	4.82*	−1	−.08	2.06
Ripl → Rspl	20.51	.00	3	14.51	.58	.24	.41	.25 - .58	15.66*	−1	−.42	18.81
FHN best fit	.11	.95	2	−3.89	1.00	.01	.00	.00 - .15	--	--	--	--
Lmfg → Rmfg	4.50	.21	3	−1.50	.96	.11	.14	.00 - .38	3.51	−1	−.04	2.39
Rspl → Rmfg	7.00	.07	3	1.00	.90	.23	.23	.00 - .45	35.74*	−1	−.10	4.89
Ripl → Rspl	--	--	0	--	--	--	--	--	--	--	--	--
Rspl → Lmfg	4.70	.20	3	−1.30	.96	.11	.15	.00 - .39	11.09*	−1	−.04	2.59
FHP best fit	2.12	.35	2	−1.88	1.00	.01	.05	.00 - .41	--	--	--	--
Lmfg → Rmfg	4.01	.26	2	−1.99	.98	.10	.12	.00 - .38	1.52	−1	−.02	−.11
Rspl → Rmfg	9.84	.02	2	3.84	.78	.26	.32	.11 - .53	7.63*	−1	−.22	5.72
Ripl → Rspl	--	--	0	--	--	--	--	--	--	--	--	--
Rspl → Lmfg	9.79	.02	2	3.79	.78	.19	.31	.11 - .53	5.47*	−1	−.22	5.67

Lmfg=Left middle frontal gyrus; Rmfg=Right middle frontal gyrus; Rspl=Right superior parietal lobule; Ripl=Right inferior frontal gyrus; Ripl=Right inferior parietal lobule

*Statistically significant ΔS-Bχ^2 p<.05

¥S-B = corrected values.